Analytical and Bioanalytical Chemistry (2018) 410:7121–7133
https://doi.org/10.1007/s00216-018-1313-2

RESEARCH PAPER

Lipidomic differentiation of Graves' ophthalmopathy in plasma and urine from Graves' disease patients

Seul Kee Byeon[1] · Se Hee Park[2,3] · Jong Cheol Lee[1] · Sena Hwang[4] · Cheol Ryong Ku[5,6] · Dong Yeob Shin[5,6] · Jin Sook Yoon[7] · Eun Jig Lee[3,5,6] · Myeong Hee Moon[1]

Received: 9 May 2018 / Revised: 31 July 2018 / Accepted: 7 August 2018 / Published online: 22 August 2018

Abstract

Approximately 50% of patients with Graves' disease (GD) develop retracted eyelids with bulging eyes, known as Graves' ophthalmopathy (GO). However, no simple diagnostic blood marker for distinguishing GO from GD has been developed yet. The objective of this study was to conduct comprehensive profiling of lipids using plasma and urine samples from patients with GD and GO undergoing antithyroid therapy using nanoflow ultrahigh performance liquid chromatography electrospray ionization tandem mass spectrometry. Plasma ($n = 86$) and urine ($n = 75$) samples were collected from 23 patients with GD without GO, 31 patients with GO, and 32 healthy controls. Among 389 plasma and 273 urinary lipids that were structurally identified, 281 plasma and 191 urinary lipids were quantified in selected reaction monitoring mode. High-abundance lipids were significantly altered, indicating that the development of GD is evidently related to altered lipid metabolism in both plasma and urine. Several urinary lysophosphatidylcholine species were found to be increased (3- to 10-fold) in both GD and GO. While the overall lipid profiles between GD and GO were similar, significant changes (area under receiver operating curve > 0.8) in GO vs. GD were observed in a few lipid profiles: 58:7-TG and (16:1,18:0)-DG from plasma, 16:1-PC and 50:1-TG from urine, and d18:1-S1P from both plasma and urine samples. An altered metabolism of lipids associated with the additional development of ophthalmopathy was confirmed with the discovery of several candidate markers. These can be suggested as candidate markers for differentiating the state of GO and GD patients based on plasma or urinary lipidomic analysis.

Keywords Graves' disease · Ophthalmopathy · Lipidomic analysis · Plasma · Urine · nUPLC-ESI-MS/MS

Seul Kee Byeon and Se Hee Park contributed equally to this work.

Electronic supplementary material The online version of this article (https://doi.org/10.1007/s00216-018-1313-2) contains supplementary material, which is available to authorized users.

✉ Eun Jig Lee
ejlee423@yuhs.ac

✉ Myeong Hee Moon
mhmoon@yonsei.ac.kr

[1] Department of Chemistry, Yonsei University, 50 Yonsei-ro, Seodaemun-gu, Seoul 03722, South Korea

[2] Division of Endocrinology and Metabolism, Department of Internal Medicine, National Health Insurance Service Ilsan Hospital, Goyang, Gyeonggi 10444, South Korea

[3] Graduate School, Yonsei University College of Medicine, 50-1 Yonsei-ro, Seodaemun-gu, Seoul 03722, South Korea

[4] Department of Internal Medicine, Chaum Life Center, CHA University School of Medicine, Seoul 06062, South Korea

[5] Division of Endocrinology and Metabolism, Department of Internal Medicine, Yonsei University College of Medicine, 50-1 Yonsei-ro, Seodaemun-gu, Seoul 03722, South Korea

[6] Institute of Endocrine Research, Yonsei University College of Medicine, 50-1 Yonsei-ro, Seodaemun-gu, Seoul 03722, South Korea

[7] Department of Ophthalmology, Yonsei University College of Medicine, 50-1 Yonsei-ro, Seodaemun-gu, Seoul 03722, South Korea

Abbreviations

ApoAV	Apolipoprotein AV
Cer	Ceramides
CID	Collision-induced dissociation
DG	Diacylglycerol
GD	Graves' disease
GO	Graves' ophthalmopathy
IS	Internal standard
LPC	Lysophosphatidylcholine
LPE	Lysophosphatidylethanolamine
MS	Mass spectrometry
nUPLC-ESI-MS/MS	Nanoflow ultrahigh performance liquid chromatography-electrospray ionization tandem mass spectrometry
PC	Phosphatidylcholine
PG	Phosphatidylglycerol
PL	Phospholipid
SL	Sphingolipid
S1P	Sphingosine-1-phosphate
TSH	Thyroid-stimulating hormone
TSI	Thyroid-stimulating immunoglobulin
T4	Thyroxine
T3	Triiodothyronine
UPLC	Ultrahigh performance liquid chromatography
VLDL	Very low-density lipoproteins

Introduction

Graves' disease (GD) is an autoimmune disease involving a dysfunctional thyroid in which thyroid-stimulating immunoglobulins (TSI) stimulate the synthesis of the thyroid hormones triiodothyronine (T3) and thyroxine (T4) [1]. The overproduction of T3 and T4 inhibits the release of thyroid-stimulating hormone (TSH) [2]. GD is conventionally diagnosed with clinical symptoms and signs resulting from hyperthyroidism, thyroid function tests, and thyrotropin receptor antibodies test [3]. Common symptoms of GD include fatigue, weight loss, tachycardia, and heat intolerance [4]. Approximately 50% of patients with GD develop Graves' ophthalmopathy or orbitopathy (GO), a condition characterized by an increase in the volume of orbital and periorbital connective tissue and fat, resulting in eyelid retraction and exophthalmos [5, 6]. Since elevated thyroid hormone levels are found in both GD patients with and without eye symptoms, the diagnosis of GO is mainly based on eye examination. There is currently no simple blood diagnostic marker capable of diagnosing ophthalmopathy among patients with GD.

Researchers over the last decades have shown that lipids are important in determining the physiology and pathophysiology of diseases [7, 8]. Since lipids play important roles in signal transduction, cell proliferation, and apoptosis, the changes in lipid levels are correlated with the progression of various metabolic diseases. Therefore, studies regarding the perturbed metabolism of lipids are crucial in diagnostic and prognostic applications. However, lipids are complex mixtures of various lengths of fatty acids with different degrees of unsaturation and types of head groups, comprising different classes of lipids, such as phospholipid (PL), sphingolipid (SL), and acylglycerol, that are known to uniquely regulate different aspects of cellular function [9–13]. Discovering the enigmatic relationship between pathophysiology and lipids requires an accurate and complete profiling of lipids. While mass spectrometry (MS) strictly provides an accurate determination of lipid molecular structures, chromatographic separation prior to MS detection is necessary to differentiate complex lipid mixtures. The recently developed state-of-the-art ultrahigh performance liquid chromatography (UPLC), coupled with MS, has been powerfully utilized to qualitatively and quantitatively analyze lipids from various types of biological samples [14, 15]. Moreover, the use of nanoflow provides an improved detection limit of ~ 1 fmol and enhanced chromatographic resolutions with reduced consumption of solvents and samples [16, 17].

Most studies on thyroid disease have focused on the levels of lipoproteins, lipoprotein lipase, cholesterol, or proteins; however, studies involving the lipidomic analysis of plasma and urine samples of patients with GD and GO are currently limited [18, 19]. In this study, qualitative and quantitative profiling of lipids from plasma and urine samples of patients with GD and GO were performed in comparison to those of healthy controls using nanoflow ultrahigh pressure liquid chromatography tandem mass spectrometry (nUPLC-ESI-MS/MS). The studies were conducted firstly with global identification of lipid molecular structures from patients' plasma and urine samples, followed by primary quantification of lipids from each pooled sample in which lipids showing significant variation (> 1.5-fold change compared to controls) were selected. Subsequently, the selected lipids were analyzed again by high-speed targeted quantification of individual samples. Lipids showing significant changes in patients with GD and GO were statistically mined to elucidate lipidomic differences in comparison to healthy controls and to differentiate additional ophthalmopathy from GD.

Experimental

Materials and reagents

The 41 lipid standards [16:0-lysophosphatidylcholine (LPC), 17:0-LPC, 13:0/13:0-phosphatidylcholine (PC), 16:0/16:0-PC, 14:0-lysophosphatidylethanolamine (LPE), 17:1-LPE, 18:0-LPE, 17:0/17:0-phosphatidylethanolamine (PE), 18:0/

20:6-PE, 18:0p/22:6-PE plasmalogen, 14:0-lysophosphatidylglycerol (LPG), 17:1-LPG, 18:0-LPG, 12:0/12:0-phosphatidylglycerol (PG), 15:0/15:0-PG, 16:0/16:0-PG, 16:0/18:2-phosphatidylinositol (PI), 17:0/20:4-PI, 17:1-lysophosphatidylserine (LPS), 18:0-LPS, 14:0/14:0-phosphatidylserine (PS), 17:0/20:4-PS, 12:0/12:0-lysophosphatidic acid (LPA), 17:0/17:0-phosphatidic acid (PA), 18:0/18:0-PA, d17:1-sphingosine-1-phosphate (S1P), d18:1-S1P, d17:1-lysosphingomyelin (LSM), d18:1-LSM, d18:1/17:0-sphingomyelin (SM), d18:1/24:0-SM, d18:1/17:0-ceramide (Cer), d18:1/22:0-Cer, d18:1/16:0-monohexosylceramide (MHC), d18:1/17:0-MHC, d18:1/16:0-dihexosylceramide (DHC), d18:1/17:0-DHC, 16:0/18:1-diacylglycerol (DG), 17:0/17:0-D_5-DG, 17:0/17:1/17:0-D_5-triacylglycerol (TG), and 18:0/18:0/18:1-TG] were purchased from Avanti Polar Lipids, Inc. (Alabaster, AL, USA) and Matreya, LLC (State College, PA, USA). The standard lipids with odd numbered fatty acyl chains were used as a mixture of internal standard (IS) to compensate for the fluctuation in mass spectrum (MS) intensity across the samples. High-performance liquid chromatography (HPLC)-grade CH_3OH, H_2O, CH_3CN, isopropanol (IPA), and methyl *tert*-butyl ether (MTBE) were purchased from Avantor™ Performance Materials (Center Valley, PA), while CH_3Cl, formic acid (FA), and NH_4HCO_2 were purchased from Sigma-Aldrich (St. Louis, MO, USA). Fused silica capillary tubing with inner diameter (I.D.) of 20, 50, and 100 μm and outer diameter (O.D.) of 360 μm were obtained from Polymicro Technology, LLC (Phoenix, AZ, USA).

Plasma and urine samples

Plasma and urine samples were obtained from 54 patients with GD who visited the endocrine clinic at the Severance Hospital, Seoul, South Korea, from October 2014 to January 2016 and 32 healthy volunteers. The diagnosis of GD was confirmed by thyroid function tests and thyrotropin receptor antibodies, and the severity of ophthalmopathy was assessed using an exophthalmometer, clinical activity scores [6], and the modified NOSPECS classification [20] by ophthalmologists, at the time of sample collection. Plasma (32 controls, 23 GD, and 31 GO) and urine (25 controls, 22 GD, and 28 GO) samples from the same individuals were obtained. All participants were enrolled into the study after providing informed consent, and the study protocol was approved by the Institutional Review Board of the Severance Hospital, South Korea (IRB No. 4-2014-0520). The clinical data of the patients (i.e., age, sex, clinical symptoms, thyroid function status, thyroid autoantibodies, and thyroid medication history) are listed in Table S1 in the Electronic Supplementary Material (ESM). Sample collection and clinical assessments are described in the ESM.

Lipid extraction from plasma and urine samples

For untargeted and semi-quantitative lipidomic analyses, both plasma and urine samples were pooled by each group (pooled controls, pooled GD, and pooled GO) to a final volume of 100 μL and 1 mL, respectively. For individual quantitative analyses, lipid extraction protocols were conducted for each individual sample. The protocols of Folch method modified with MTBE/CH_3OH were applied to both plasma and urine samples for lipid extraction except that 100 μL of raw plasma was used while 1 mL of urine was lyophilized for 12 h prior to the extraction due to its large volume [21]. To raw plasma and lyophilized urine, 300 μL of HPLC-grade CH_3OH was added and then mixed by shaking. After shaking, 1000 μL of MTBE was added and shaken for an hour. For phase separation between aqueous and organic layers, 250 μL of HPLC-grade H_2O was added and vortexed for 10 min, followed by centrifugation at 1000×*g* for 10 min. The upper organic phase was pipetted and saved while 400 μL of MTBE:CH_3OH (10:3, *v*/*v*) was added to the remaining lower layer and tip-sonicated for 2 min. After centrifuging at 1000×*g* for 10 min, the supernatant was collected and combined with the previously collected organic layer, followed by lyophilization for 12 h. During lyophilization, the open tops of all sample tubes were wrapped with 0.45 μm MillWrap PTFE membrane from Millipore (Bedford, MA, USA). Lyophilized lipid extract was reconstituted in $CHCl_3$:CH_3OH(3:7, *v*/*v*) and diluted using CH_3OH:H_2O (9:1, *v*/*v*) to 5 μg/μL for plasma and 15 μg/μL for urinary lipids. All samples were maintained at − 87 °C for further analysis by nanoflow ultrahigh performance liquid chromatography electrospray ionization tandem mass spectrometry (nUPLC-ESI-MS/MS).

Lipid analysis using nUPLC-ESI-MS/MS

Two different processes of nUPLC-ESI-MS/MS were employed for untargeted identification of lipids from pooled samples and targeted quantification (both pooled and individual samples). For untargeted analysis, Thermo Scientific™ UltiMate™ 3000 RSLCnano System was coupled to Thermo LTQ Velos ion trap mass spectrometer [both purchased from Thermo Fisher Scientific (Waltham, MA, USA)]. However, nanoACQUITY UPLC from Waters (Milford, MA, USA) with TSQ Vantage triple-stage quadrupole MS from Thermo Fischer Scientific was utilized for selected reaction monitoring (SRM) quantification of pooled and individual lipid samples. For all analyses, a 7-cm-long pulled-tip capillary column (100 μm × 360 μm, I.D. × O.D.) was prepared by packing with 1.7 μm ethylene bridged hybrid (BEH) C18 resin in the laboratory. For lipid quantification, the SRM method was utilized, and the type of precursor and quantifier ions of each lipid category are listed in ESM Table S3. Prior to the plasma and urinary lipid analysis, the

efficiency of different types of modifiers added to mobile phase solution for nUPLC-ESI-MS/MS detection was firstly evaluated to detect a broad spectrum of lipids ranging from S1P to TG. A modifier condition, 1 mM ammonium formate (AF) with 1% FA, was chosen as the most effective ionization modifier in this analysis because the ionization efficiency for most classes of lipids, including S1P, was > 85%. Variations in ionization efficiency with different modifiers are described in detail further in this text. For all analyses, a 7-cm-long analytical column was prepared in the laboratory by pulling one end of capillary tubing (100 μm × 360 μm, I.D. × O.D.) to a sharp needle using a flame torch. Under nitrogen gas at 1000 psi, the pulled-tip capillary column was packed with 1.7 μm BEH C18 resin, which was unpacked from XBridge® BEH C18 (1.7 μm, 2.1 mm × 100 mm) of Waters, in a methanol slurry. However, in order to avoid 1.7 μm-sized particles from eluting out of the capillary column during the LC-MS run, the needle tip (5 mm) was packed with 3 μm-sized Watchers® ODS-P C18 resin, purchased from Isu Industry Corp. (Seoul, South Korea). The analytical column was connected to the LC pump via capillary tubing through a PEEK MicroCross from IDEX (Oak Harbor, WA); one of the other ends of MicroCross was deployed with platinum wire for electrical source, while the last one was extended out to a split valve via another capillary tubing. The split valve was closed on and off during elution and sample loading, respectively, to apply the binary gradient change faster at tens of μL/min during elution, and a capillary tubing was attached to the split valve to adjust the split flow. Two types of mobile phases [mobile phase A consisted of H_2O:CH_3CH (9:1, *v*/*v*) and mobile phase B of IPA:CH_3OH:CH_3CN (6:2:2, *v*/*v*/*v*)] were utilized in binary gradient elution, and both mobile phases contained a mixed modifier of a 1 mM NH_4HCO_2 with 1% FA for a simultaneous analysis of PLs, AGLs, and SLs, including S1P.

For untargeted lipidomic analysis, the sample was loaded to the analytical column using mobile phase A 99% (mobile phase B 1%) at a flow rate of 600 nL/min for 13 min with the split valve closed. In positive ion mode, the mobile phase B was ramped to 70% over 2 min with the split valve open at an increased flow rate of 6 μL/min, in which only 300 nL/min was delivered to the analytical column while the remaining flow exited through via split tubing at the MicroCross. Then, mobile phase B was raised to 85% over the next 5 min, 90% over 5 min, 99% over 5 min, and then maintained at 99% for 12 min. In negative ion mode, the mobile phase B was ramped to 75% over 2 min, 80% over 6 min, 95% over 9 min, and then 99% over 9 min. The mobile phase B was maintained at 99% for 10 min. After each run, the analytical column was equilibrated with mobile phase A for 10 min. All samples were analyzed in triplicate runs with an injection of 2 μL (equivalent to 10 and 30 μg of dried lipid extracts for plasma and urine, respectively) with 1 pmol of IS mixtures (17:0-LPC, 13:0/13:0-PC, 17:1-LPE, 17:0/17:0-PE, 17:1-LPG, 15:0/15:0-PG, 17:0/20:4-PI, 17:1-LPS, 17:0/20:4-PS, 17:0/17:0-PA, d17:1-S1P, d17:1-LSM, d18:1/17:0-SM, d18:1/17:0-Cer, d18:1/17:0-MHC, d18:1/17:0-DHC, 17:0/17:0-D_5-DG, 17:0/17:1/17:0-D_5-TG) per run, in both negative and positive ion modes. The IS mixture was added to the samples accordingly right before the injection for the nUPLC-ESI-MS/MS so the equal amount of IS mixture (1 pmol) would be injected. All lipids were structurally identified based on data-dependent collision-induced dissociation (CID) spectra; LPC, PC, LPE, PE, DG, and TG were identified in positive ion mode, while the remaining classes of lipids were identified in negative ion mode. The structures of Cer, SM, MHC, DHC, and THC were determined in MS^3 analysis of negative ion mode while other lipids were determined in MS^2 analysis. A precursor range of *m/z* 300–1200 for negative ion mode and *m/z* 300–1000 for positive ion mode at 3.0 kV of ESI with 40% of normalized collision energy was applied in the analysis. For the structural determination of lipids, LiPilot, a software algorithm for identification of lipids based on spectral libraries of lipids, was used followed by manual confirmation [22].

Structural analysis of lipids based on CID spectra resulted in the identification of 389 lipids from plasma (16 LPC, 39 PC, 7 LPE, 20 PE, 13 PEp, 6 LPG, 22 PG, 2 LPI, 20 PI, 5 PA, 1 S1P, 4 LSM, 23 SM, 13 Cer, 9 MHC, 4 DHC, 4 THC, 23 DG, and 158 TG) and 273 lipids from urine (7 LPC, 26 PC, 3 LPE, 13 PE, 7 PEP, 3 LPG, 11 PG, 1 LPI, 16 PI, 1 LPS, 10 PS, 5 PA, 1 S1P, 4 LSM, 21 SM, 8 Cer, 7 MHC, 5 DHC, 4 THC, 10 DG, and 110 TG) as listed in ESM Table S2. Based on untargeted lipidomic analysis, targeted lipids from 10 to 30 μg of dried lipid extracts for plasma and urine samples, respectively, were quantified using SRM mode with 1 pmol of IS mixture (the same mixture that was used for untargeted analysis), which was added to each and every sample accordingly right before the injection for the nUPLC-ESI-MS/MS so the equal amount of IS mixture (1 pmol) would be analyzed across all samples. All samples were mixed with a mixture of IS, which contained various classes of lipids with odd numbered carbons in their fatty acyl chains because they were not found in human samples. In order to compensate for the time required for calculating the peak areas of many lipids from a large sample set, semi-quantification from pooled samples was conducted at first and lipid species that showed strong potential for producing a significant difference between the groups (> 1.5-fold included with standard deviation) were selected. The selected lipids were specifically analyzed individually for quantitation and for evaluating the distribution within the group and statistical significance. A mixture of IS was mixed with samples in both pooled and individual quantitative analysis and the same elution gradient in LC was applied. The sample was loaded to the column using mobile phase A for 10 min at 1 μL/min with the split valve closed. For separation of lipids, mobile phase B was ramped to 50% over 1 min, 80% over 3 min, 100% over 9 min, and then maintained at 100%

for 8 min. During separation, the flow rate was set at 20 μL/min with the split valve open and only 300 nL/min was delivered to the column. Collision energy assigned to each class of lipids and forms of precursor ion with product ions are listed in ESM Table S1. The scan time was set at 0.001 s, scan width at *m/z* 1.0, and ESI voltage at 3 kV. Unlike the untargeted analysis in which separate runs in each positive and negative ion modes were conducted, alternating ion modes in one run was performed in quantitative analysis in the SRM mode in order to analyze all lipids in one run.

Statistical analysis

Continuous variables are expressed as mean ± standard deviation. Student's *t* tests were used for the analysis of continuous variables to compare the baseline characteristics of the GO and GO groups. Categorical variables, such as gender or thyroid function status, were analyzed using chi-square tests. *p* values < 0.05 were considered statistically significant. Statistical analysis was performed using SPSS version 23 (IBM Corp., Armonk, NY, USA). For quantitative analysis of lipids, Student's *t* test and principal component analysis (PCA) were evaluated through Minitab 17 software (Minitab, Inc., State College, PA, http://www.minitab.com).

Results and discussion

Effect of ionization modifiers on lipid analysis

Formic acid (FA) is widely used for the detection of lipids in positive ion mode of MS, and ammonium hydroxide or ammonium formate (AF) for negative ion mode. AF in general enhances the stability of C18, reversed phase LC packing materials, in basic condition [23]. The effect of four different types of modifiers (1 mM AF, 1 mM AF with 0.1% FA, 1 mM AF with 1% FA, and 5 mM AF with 1% FA) on MS intensity lipid standards was evaluated in SRM mode of nUPLC-ESI-MS/MS. Relative MS intensity (%) of the various classes of PLs, SLs, and AGLs is compared in ESM Fig. S1. The percentages are relative to the highest peak intensity of one of the four modifiers tested for each class of lipids across all classes. For instance, as the MS intensity of LPC was the highest when 5 mM AF with 1% FA were used, relative MS intensity of LPC is indicated as 100% for 5 mM AF with 1% FA. However for PC, the highest signal was observed when 1 mM AF with 1% FA was used. Therefore, we indicated the relative MS intensity of PC to be 100% for 1 mM AF with 1% FA. Although 1 mM AF yielded higher MS intensities for lipids, such as LPG, PG, PI, and others > 1 mM AF with 1% FA, S1P was not detected at all when FA was not present as an ionization modifier. In fact, S1P could not be detected if mobile phases contained only 0.1% of FA; however, S1P was readily detected when FA was increased to 1%. As AF was increased to 5 mM from 1 mM with 1% FA, the MS intensity of most classes decreased, indicating that 1 mM AF is more effective than 5 mM AF. The average ionization efficiency (%) across all classes of lipids was 84.1% for 1 mM AF with 0.1% FA, 90.8% for 1 mM AF with 1% FA, 72.5% for 5 mM AF with 1% FA, and 91.1% for 1 mM AF alone. Although 1 mM AF with 1% FA was outperformed by 1 mM AF, their difference in efficiency was negligibly small (0.3%) and the presence of FA was crucial for the detection of S1P. As the ionization efficiency of 1 mM AF with 1% FA for most classes of lipids was > 85%, 1 mM AF with 1% FA was chosen as the most effective ionization modifier in this analysis.

Structural determination of lipids

The base peak chromatograms of various lipid standards and the plasma and urinary lipids of pooled controls, obtained from the lipid analysis using nUPLC-ESI-MS/MS, are shown in ESM Fig. S2 and S3, respectively. Using 1 mM AF with 1% FA as the ionization modifier, most lipid classes (i.e., PLs, SLs, and AGLs) were readily identified with their molecular structures based on data-dependent CID experiments using nUPLC-ESI-MS/MS (ion trap) as reported in earlier studies [14, 15, 24]. In the cases of d18:1-S1P and d18:1-lysosphingomyelin (LSM), these could be analyzed in both positive and negative ion modes, with protonated ($[M+H]^+$) and deprotonated ($[M-H]^-$) forms, respectively (Fig. 1). For S1P, characteristic fragments resulting from the loss of H_2O (*m/z* 362.4, $[M+H-H_2O]^+$), phosphate group (*m/z* 282.4, $[M+H-H_3PO_4]^+$), and phosphate group with H_2O (*m/z* 264.4, $[M+H-H_3PO_4-H_2O]^+$) were observed in positive ion mode under a collision energy of 40 eV, while deprotonated phosphate ion was observed after the loss of H_2O (*m/z* 79, $[H_2PO_4-H_2O]^-$) in negative ion mode under 20 eV (Fig. 1a, b). However, under a collision energy of 40 eV, which was found to be the optimized collision energy for data dependent analysis, the dominant fragment of $[H_2PO_4-H_2O]^-$ disappeared, making it difficult for S1P to be analyzed in negative ion mode during untargeted identification of lipids by nUPLC-ESI-MS/MS. Moreover, as the intensities of fragments during MS^2 were substantially higher in positive ion mode, S1P was analyzed in positive ion mode throughout the study. For LSM, protonated ($[M+H]^+$) and formate adduct ($[M+HCO_2]^-$) forms of standard d18:1-LSM were obtained. MS^2 analysis of these precursor ions yielded prominent fragments of protonated phosphocholine at *m/z* 184 and loss of H_2O at *m/z* 447.4 in positive ion mode (Fig. 1c) or $[M-CH_3]^-$ in negative ion mode. Additional CID analysis of $[M-CH_3]^-$ yielded fragments (Fig. 1d) *m/z* 378.4 and 360.4 by dissociation of the choline group from $[M-CH3]^-$ in the form of -$CH_2CHN(CH_3)_2$ with and without loss of the hydroxyl group by dehydration, respectively. Due to the detection of highly

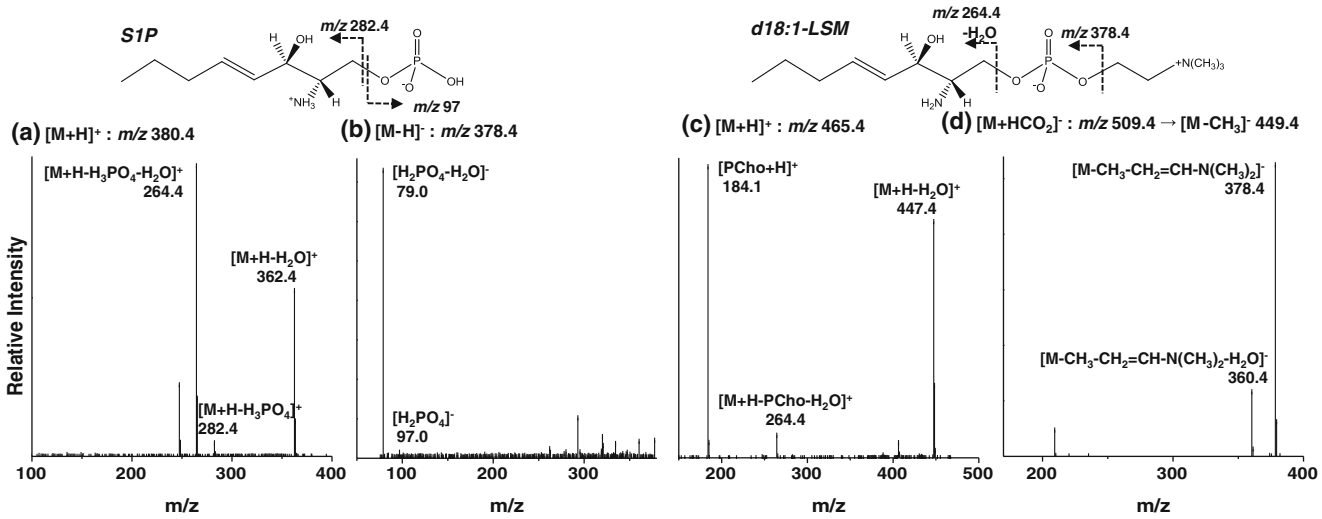

Fig. 1 MS^2 spectra of S1P standard in (**a**) positive and (**b**) negative ion mode (collision energies of 40 and 20 eV, respectively). (**c**) MS^2 spectra of d18:1-LSM in positive and (**d**) MS^3 in negative ion mode, both at a collision energy of 40 eV, are also shown. All spectra are obtained using LTQ Velos ion trap mass spectrometer. S1P, sphingosine-1-phosphate; LSM, lysosphingomyelin

prominent *m/z* 184, analysis can be facilitated in positive ion mode. Structural analysis of lipid based on CID spectra facilitated the identification of 389 lipids from plasma (16 LPC, 39 PC, 7 LPE, 20 PE, 13 PEP, 6 LPG, 22 PG, 2 LPI, 20 PI, 5 PA, 1 S1P, 4 LSM, 23 SM, 13 Cer, 9 MHC, 4 DHC, 4 THC, 23 DG, and 158 TG) and 273 lipids from urine (7 LPC, 26 PC, 3 LPE, 13 PE, 7 PEP, 3 LPG, 11 PG, 1 LPI, 16 PI, 1 LPS, 10 PS, 5 PA, 1 S1P, 4 LSM, 21 SM, 8 Cer, 7 MHC, 5 DHC, 4 THC, 10 DG, and 110 TG). The molecular structures of identified lipids are listed with quantification results in ESM Table S2; the numbers inside the parentheses with "P" and "U" represent the number of lipids found from plasma (P) and urine (U) samples, respectively. LPS and PS were identified from urine only.

Untargeted and semi-quantitation of plasma and urinary lipids

The identified lipids were first quantified from pooled samples to select species for high-speed quantification of individual samples mainly using the selected reaction monitoring (SRM) mode of nUPLC-ESI-MS/MS. All lipids were quantified by calculating and correcting the relative peak areas of each lipid to those of their corresponding class of the IS (1 pmol for each class). The corrected peak areas of plasma and urinary lipids from the pooled samples are listed in ESM Table S2, and the types of precursor/quantifier ions for quantifying each lipid class are listed in ESM Table S3, with additional details of the SRM method in the ESM. As triglycerides (TGs) were quantified without differentiating the isomers, the possible acyl chains identified from the CID spectra are listed in ESM Table S4. The relative abundance of lipids was calculated by the peak area percentage (%) of each lipid with respect to the sum of peak areas of all lipids within the corresponding class of healthy controls. If the relative abundance was higher than the average abundance (100%/number of lipids within the class), the species was regarded as a high abundance lipid in this study. High abundance lipids are underlined in ESM Table S2 under the "Abun." column. The numbers of lipids that were highly abundant in plasma were found to be highly abundant in urine as well, except for phosphatidylglycerol (PG), suggesting that the metabolism of plasma PG may differ from that of urinary PG, although the factors triggering such change are unknown.

The fold change of overall lipids in GD and GO in comparison to healthy controls was examined by adding the peak areas of all lipid species within the corresponding class of lipids. The significant (> 1.5-fold change and $p < 0.001$, significant values are marked with an asterisk) and non-significant classes are shown in ESM Fig. S4a and S4b, respectively. While the changes in plasma lysophosphatidylcholine (LPC) level in GD and GO were not significant, urinary LPC levels increased by 6.6-fold for GD and 7.4-fold for GO. Contrary to the increase in urinary LPC levels, urinary PC levels significantly decreased by approximately 1.5-fold. The decrease in lysophosphatidylethanolamine (LPE) levels in the GO group was observed in both plasma and urine samples. Plasma levels of ceramides (Cer) significantly decreased in both GD and GO groups by 1.9-fold, but the decreases in urinary levels were negligible. While the plasma levels of Cer decreased in both GD and GO groups, the plasma and urinary S1P levels increased. S1P and Cer are reported to play opposite roles in cellular function. S1P is associated with cell growth, differentiation, and migration, while Cer is related to cell death and growth arrest [25–27]. Apoptotic Cer decreased with increasing cell growth-related S1P levels in both plasma and urine

samples in the GD and GO groups. The elevated S1P level can be partially attributed to the decreased Cer level through the SL pathway, hydrolysis of ceramide produces sphingosine, and phosphorylation of sphingosine by sphingosine kinase 1 and 2 to form S1P.

Statistical evaluations among GO and GD groups vs. controls

Based on the quantitative analysis of pooled samples, lipids showing alterations (> 1.5-fold) in patients with GD and GO in comparison to controls (C) were selected for targeted quantification of individual samples and their results are compared in ESM Table S5 with fold changes in GD/C, GO/C, and GO/GD. The "blank" boxes represent the lipids that were not selected for individual analysis because their levels were not greatly altered in the pooled analysis. Species with > 1.5-fold change ($p < 0.01$) are shown in bold font, while those with a > 2-fold change are underlined. The principal component analysis plots in Fig. 2 were based upon lipids with a > 1.5-fold change, and the individual points represent the overall lipid level of the individual. Although a few patients with GO overlapped with patients with GD, individuals within each group were well clustered. The cluster of GO was positioned further away from the control group for both plasma and urinary lipid levels, which implies that the GO group differs from controls than GD. In addition, the overlapped region of GD and GO was larger in urine than plasma samples; therefore, the overall degree of difference between urinary lipids of GD and GO was not as large as that of plasma.

The lipids that showed a > 2-fold change ($p < 0.01$) were identified, analyzed via receiver operating characteristic analysis, and the resulting species with an area under curve (AUC) > 0.8 are listed in Table 1. The distinct difference among the groups was evidently observed through the *Z*-score heat map (Fig. 3). A unique phenomenon that was observed was the fold change in plasma and urinary TG (Table 1). GD is characterized by hyperthyroidism because excessive thyroid hormones are synthesized. Similar to a study in which unchanged or slightly low TG levels were reported among patients with hyperthyroidism [19], the overall level of total urinary TG in the GD and GO groups (ESM Fig. S4) was similar to healthy controls. In contrast, increased TG levels were observed from plasma samples, which can be explained as follows. None of the species that increased significantly in plasma were high abundance lipids; therefore, the overall TG level was not notably affected (the overall fold change in plasma TG was 1.14-fold in the GD group and 1.16-fold in the GO group). However, the low level of TG in hyperthyroidism was directly related to the levels of T3 because T3 is purported to induce the synthesis of apolipoprotein AV (ApoAV) [28]. High levels of T3 are one of the hallmark features of GD; therefore, ApoAV levels are elevated in patients with GD, which decreases the production of TG from very low-density lipoproteins (VLDL) by enhancing lipoprotein lipase [29]. Therefore, lipoprotein lipase induces the lipolysis of VLDL-derived TG and subsequently lowers TG levels. However, in this study, the patients with GD and GO were undergoing antithyroid drug treatment and their T3 levels recovered to nearly normal levels (only three and two patients from the GD and GO groups, respectively, had abnormally high levels of T3). This could partially affect the expected result of decreased TG levels.

Moreover, among the lipid species with significant changes (AUC > 0.800; Table 1), urinary 16:1-LPC exhibited an AUC > 0.800 in all three comparisons: 0.940 for GD vs. C, 0.997 for GO vs. C, and 0.884 for GO vs. GD (ESM Fig. S5). Although there was a 1.68-fold change between GO and GD, the statistical evaluation between the GO and GD groups was significantly different. The increased LPC species are known biomarker molecules of metabolic diseases, such as cardiovascular disease, and therefore, their elevation often indicates disease progression [30]. In this study, all plasma and urinary LPC species were increased in GD and GO, which clearly implied the pathological state of patients. Regarding the thyroid function status, most patients were euthyroid or had subclinical hypo- or hyperthyroidism with antithyroid drug treatment, and these changes in LPC species might be associated with thyroid autoimmunity. The increase in urinary LPC levels was especially remarkable because all seven urinary LPC species were found to increase significantly in GD and GO. The overall and individual fold changes of urinary LPC calculated from the individual analysis are shown (Fig. 4a), along with the fold change of urinary PC species containing the same fatty acyl chains at the sn-1 location (Fig. 4b). In contrast to the increased level of urinary LPC, all urinary PCs containing the same fatty acyl chains decreased in GD and GO. In previous studies, it has been reported that oxidation of PLs results in the formation of lysophospholipids by cleavage of the unsaturated fatty acyl chain at the sn-2 position [31, 32]. Therefore, LPCs with 16:0, 18:0, and 18:1 can be partially attributed to the decreased levels of PC molecules with 16:0/xx:x, 18:0/xx:x, and 18:1/xx:x, respectively. Among these PL species, lipids that showed significant changes are marked with an asterisk in Fig. 4b.

From the quantitative analysis of individual samples, seven lipids were found to vary significantly (> 1.5-fold and $p <$ 0.01) in both the plasma and urine samples in the GO group only. The corrected peak area ratios (vs. IS) of individuals in the control (C) and GO groups are plotted in Fig. 5. The most significant difference was observed for urinary 16:0-LPC because none of the corrected peak areas of healthy controls overlapped with those of GO. Similar patterns of change in both plasma and urine were observed in five lipids (16:0-LPC, 18:0-LPE, 18:1-LPE, 18:0/18:2-PG, and d18:1-S1P) along

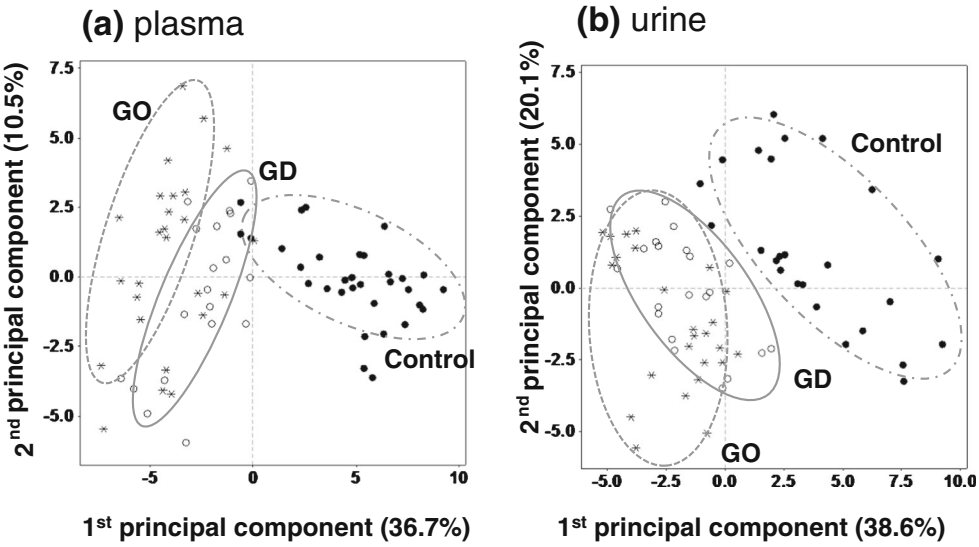

Fig. 2 Principal component analysis of selective lipids by individual analysis. Lipids from (**a**) plasma and (**b**) urine samples with significant differences (> 1.5-fold and $p < 0.01$) compared to controls are shown

with similar fold changes regarding the development of GO. In contrast, two lipids (d18:1/24:2-SM and 48:1-TG) were significantly increased in plasma samples, but decreased in urine samples.

Table 1 Selected lipids with a significant difference shown in bold (> 2-fold and $p < 0.01$) compared to healthy controls. Number of plasma/urine samples: 32/25, controls; 23/22, GD patients; and 31/28, GO patients. Underlined abundance (Abun.) % indicates relatively high-abundant species within the corresponding lipid classes. (GD, Graves' disease; GO, Graves' ophthalmopathy; C, controls; N/A, not applicable; N.D., not detected)

Classes	Molecular species	*m/z*	Plasma				Urine			
			GD/C	GO/C	GO/GD	Abun. %	GD/C	GO/C	GO/GD	Abun. %
LPC	16:0	496.4	1.44 ± 0.17	1.74 ± 0.18	1.21 ± 0.11	34.5	**9.66 ± 0.86**	**8.56 ± 0.81**	0.99 ± 0.07	23.9
	16:1	494.4	1.24 ± 0.11	1.27 ± 0.11	1.02 ± 0.12	3.2	**3.65 ± 0.34**	**6.12 ± 0.69**	1.79 ± 0.17	13.1
	18:0	524.4	1.28 ± 0.12	1.40 ± 0.11	1.09 ± 0.08	16.9	**7.68 ± 0.79**	**7.59 ± 0.84**	1.02 ± 0.10	5.3
	18:1	522.4	1.20 ± 0.11	1.31 ± 0.14	1.09 ± 0.11	10.6	**7.30 ± 0.82**	**9.99 ± 0.70**	1.33 ± 0.15	17.0
	18:2	520.4	1.20 ± 0.12	1.33 ± 0.14	1.11 ± 0.11	17.8	**6.14 ± 0.63**	**5.75 ± 0.55**	0.97 ± 0.10	27.3
	20:3	546.4	0.99 ± 0.12	1.22 ± 0.13	1.23 ± 0.16	1.4	**2.72 ± 0.24**	**2.84 ± 0.24**	0.98 ± 0.08	3.7
	20:4	544.4	1.12 ± 0.13	1.45 ± 0.17	1.29 ± 0.17	7.5	**8.90 ± 0.85**	**6.61 ± 0.69**	0.86 ± 0.09	9.7
LPE	22:6	524.4	N.D.	N.D.	N.D.	N/A	0.53 ± 0.06	**0.41 ± 0.04**	0.79 ± 0.11	32.91
PE	16:0/22:5	764.5	1.16 ± 0.12	1.00 ± 0.10	0.86 ± 0.07	7.35	**0.33 ± 0.03**	0.66 ± 0.08	1.99 ± 0.24	3.03
	16:0/22:6	762.5	**2.08 ± 0.29**	1.87 ± 0.23	0.76 ± 0.11	0.4	N.D.	N.D.	N.D.	N/A
	18:0/20:3	768.5	0.88 ± 0.07	0.84 ± 0.07	0.96 ± 0.09	19.9	**0.46 ± 0.03**	0.68 ± 0.05	1.48 ± 0.11	13.9
	18:0/20:4	766.5	1.16 ± 0.09	1.09 ± 0.08	0.94 ± 0.07	4.5	**0.39 ± 0.03**	0.70 ± 0.06	1.82 ± 0.16	9.1
	18:1/18:2	740.5	1.05 ± 0.09	0.90 ± 0.08	0.86 ± 0.06	0.4	**0.34 ± 0.03**	0.61 ± 0.07	1.79 ± 0.22	7.0
	18:1/20:4	764.5	1.21 ± 0.14	1.15 ± 0.13	0.95 ± 0.08	6.9	**0.34 ± 0.03**	0.59 ± 0.06	1.72 ± 0.21	3.0
PG	14:0/18:2	715.6	**0.44 ± 0.07**	**0.46 ± 0.05**	1.05 ± 0.21	2.3	N.D.	N.D.	N.D.	N/A
	16:0/18:2	743.6	**0.50 ± 0.07**	**0.47 ± 0.07**	0.94 ± 0.10	21.4	1.10 ± 0.09	0.84 ± 0.06	0.76 ± 0.06	6.0
	16:0/22:5	793.6	0.67 ± 0.11	0.55 ± 0.09	0.83 ± 0.10	1.9	**0.48 ± 0.05**	0.65 ± 0.05	1.35 ± 0.16	16.9
	18:0/18:2	771.6	**0.50 ± 0.07**	**0.47 ± 0.06**	0.93 ± 0.09	14.6	0.92 ± 0.11	**0.49 ± 0.06**	0.53 ± 0.06	2.8
	18:2/20:3	793.6	0.57 ± 0.08	0.57 ± 0.09	1.00 ± 0.13	3.9	1.12 ± 0.10	0.80 ± 0.09	0.72 ± 0.06	39.7
	22:6/22:6	865.6	0.61 ± 0.09	**0.47 ± 0.06**	0.78 ± 0.07	0.3	N.D.	N.D.	N.D.	N/A
PI	18:1/18:2	859.6	**0.43 ± 0.05**	**0.43 ± 0.05**	1.01 ± 0.15	5.3	1.00 ± 0.12	1.06 ± 0.15	1.06 ± 0.16	1.7
	18:1/20:4	883.6	**0.42 ± 0.05**	**0.45 ± 0.06**	1.06 ± 0.18	3.2	0.65 ± 0.07	0.83 ± 0.09	1.29 ± 0.15	1.3
S1P	d18:1	380.4	1.30 ± 0.13	**1.98 ± 0.17**	1.53 ± 0.15	100.0	1.24 ± 0.2	**1.88 ± 0.24**	1.52 ± 0.24	100.0
SM	d18:1/16:1	701.6	1.18 ± 0.13	1.01 ± 0.09	0.88 ± 0.10	3.9	**0.50 ± 0.07**	0.68 ± 0.05	1.36 ± 0.19	1.0

Table 1 (continued)

Classes	Molecular species	*m/z*	Plasma				Urine			
			GD/C	GO/C	GO/GD	Abun. %	GD/C	GO/C	GO/GD	Abun. %
Cer	d18:1/21:0	608.6	**0.44 ± 0.06**	**0.49 ± 0.07**	1.12 ± 0.18	0.1	N.D.	N.D.	N.D.	N/A
	d18:1/22:0	622.6	0.53 ± 0.04	**0.50 ± 0.05**	0.96 ± 0.07	6.5	0.81 ± 0.07	0.73 ± 0.07	0.90 ± 0.07	5.6
	d18:1/23:0	636.6	**0.47 ± 0.05**	**0.44 ± 0.04**	0.88 ± 0.06	11.1	0.89 ± 0.08	0.86 ± 0.08	0.96 ± 0.09	5.9
	d18:1/24:0	650.6	0.53 ± 0.04	**0.46 ± 0.05**	0.86 ± 0.11	44.6	0.76 ± 0.07	0.79 ± 0.07	1.04 ± 0.10	26.4
	d18:2/23:0	634.6	0.51 ± 0.10	**0.50 ± 0.08**	0.81 ± 0.14	1.2	N.D.	N.D.	N.D.	N/A
	d20:0/24:0	680.6	**0.48 ± 0.05**	**0.48 ± 0.07**	0.99 ± 0.14	0.1	N.D.	N.D.	N.D.	N/A
MHC	d18:0/24:1	812.6	0.56 ± 0.05	**0.45 ± 0.05**	1.08 ± 0.09	0.7	0.81 ± 0.07	0.97 ± 0.11	1.21 ± 0.14	0.9
	d18:1/24:0	812.6	0.80 ± 0.07	**0.50 ± 0.04**	0.78 ± 0.10	29.4	0.96 ± 0.09	0.85 ± 0.08	0.89 ± 0.08	10.5
DG	16:0,18:1	612.6	1.94 ± 0.25	**2.29 ± 0.20**	1.18 ± 0.15	0.3	1.07 ± 0.13	1.03 ± 0.09	0.96 ± 0.08	0.3
	16:0,18:2	610.6	1.64 ± 0.20	**2.01 ± 0.17**	1.22 ± 0.15	0.7	1.08 ± 0.17	1.04 ± 0.14	0.97 ± 0.13	0.1
TG	44:1	766.8	**2.04 ± 0.29**	1.33 ± 0.19	0.65 ± 0.11	0.1	N.D.	N.D.	N.D.	N/A
	44:2	764.8	**2.06 ± 0.29**	**2.99 ± 0.49**	1.45 ± 0.29	0.0	0.95 ± 0.09	0.44 ± 0.05	0.47 ± 0.05	0.2
	46:1	794.8	**2.06 ± 0.28**	1.62 ± 0.24	0.79 ± 0.14	0.3	0.68 ± 0.07	**0.45 ± 0.05**	0.67 ± 0.07	0.8
	46:2	792.8	1.53 ± 0.20	1.60 ± 0.24	1.04 ± 0.19	0.2	0.66 ± 0.07	**0.44 ± 0.05**	0.66 ± 0.08	0.5
	48:1	822.8	1.58 ± 0.16	1.63 ± 0.21	1.03 ± 0.16	0.8	0.68 ± 0.07	**0.43 ± 0.05**	0.64 ± 0.07	2.2
	50:1	850.8	1.55 ± 0.13	1.48 ± 0.16	0.95 ± 0.11	4.3	0.58 ± 0.07	**0.37 ± 0.05**	0.64 ± 0.09	2.5
	50:2	848.8	1.35 ± 0.10	1.33 ± 0.11	0.98 ± 0.10	6.4	0.59 ± 0.07	**0.39 ± 0.05**	0.66 ± 0.09	1.9
	50:3	846.8	1.39 ± 0.14	1.46 ± 0.08	1.05 ± 0.11	3.1	0.67 ± 0.08	**0.48 ± 0.05**	0.71 ± 0.08	0.9
	52:1	878.8	1.26 ± 0.09	1.38 ± 0.10	1.09 ± 0.10	1.3	0.51 ± 0.06	**0.39 ± 0.04**	0.76 ± 0.05	1.2
	54:1	906.8	1.57 ± 0.14	**2.19 ± 0.27**	1.40 ± 0.19	0.1	N.D.	N.D.	N.D.	N/A
	54:7	894.8	1.85 ± 0.24	**2.63 ± 0.36**	1.42 ± 0.24	0.5	1.06 ± 0.11	0.88 ± 0.11	0.83 ± 0.10	0.3
	54:8	892.8	**2.22 ± 0.33**	1.89 ± 0.25	0.85 ± 0.15	0.3	N.D.	N.D.	N.D.	N/A
	58:9	946.8	1.95 ± 0.28	**2.32 ± 0.33**	1.19 ± 0.21	0.4	N.D.	N.D.	N.D.	N/A
	58:10	944.8	**2.19 ± 0.31**	**2.75 ± 0.38**	1.26 ± 0.22	0.4	N.D.	N.D.	N.D.	N/A
	60:13	966.8	2.13 ± 0.30	**3.03 ± 0.46**	1.43 ± 0.27	0.0	N.D.	N.D.	N.D.	N/A

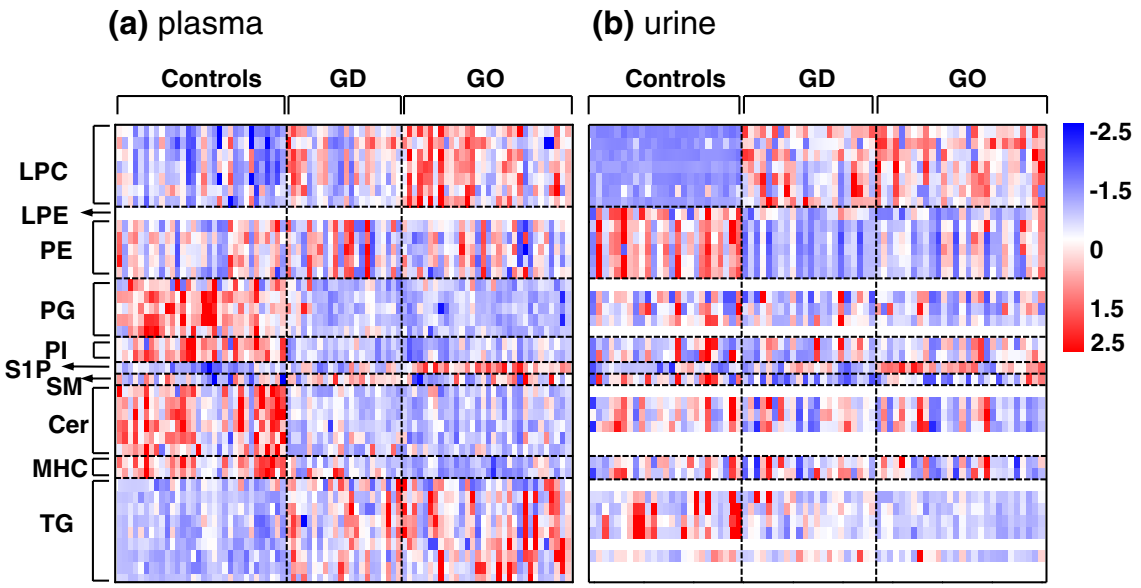

Fig. 3 Z-score heat map based on (**a**) plasma and (**b**) urinary lipids. Lipids that showed significant differences in Table 1 (> 2-fold and $p < 0.01$) among controls (•), patients with Graves' disease (GD; o), and patients with Graves' ophthalmopathy (GO; *) are included

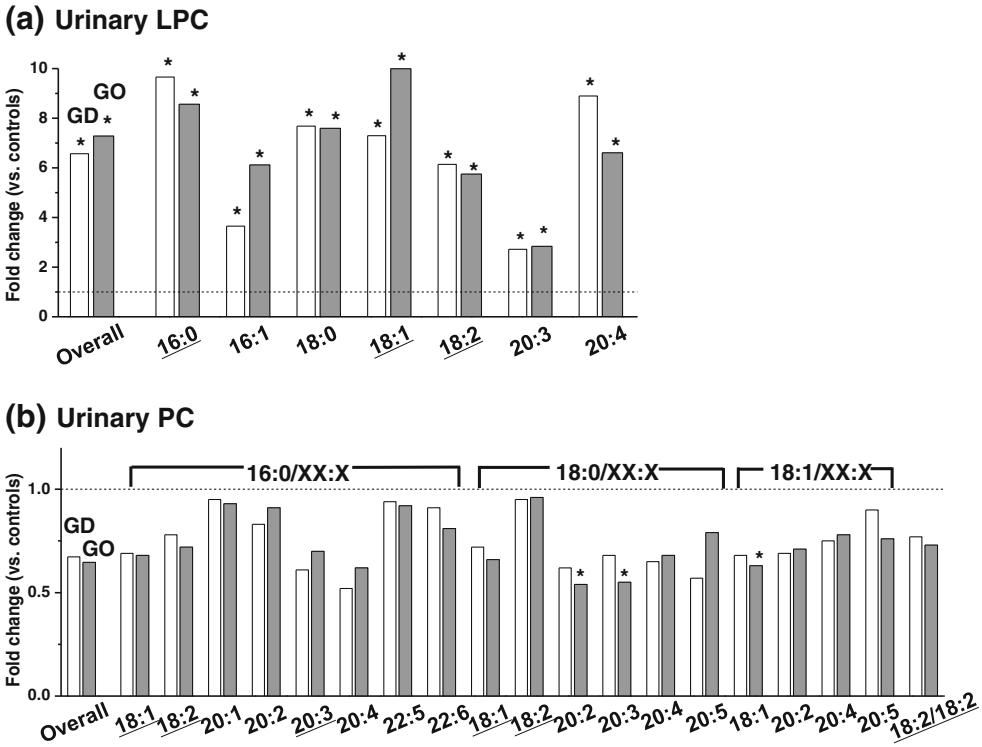

Fig. 4 Fold change of (**a**) urinary lysophosphatidylcholine (LPC) species from individual analysis and (**b**) urinary phosphatidylcholine (PC) species. The urinary PC species contained the same fatty acyl chains at the sn-1 position. Species marked with an asterisk showed significant difference (> 1.5-fold and $p < 0.01$) compared to controls and the underlined species are high abundance lipids

GO is a thyroid disorder characterized by the presence of GD along with eye disease; therefore, the overall lipidomic profiling of plasma and urine samples of patients with GO was not significantly different from that of GD. However, four and eight lipids from plasma and urine, respectively, exhibited > 1.5-fold change ($p < 0.01$) between GO and GD, proving that the additional development of eye disease is associated with further alterations of plasma and urine lipidome. The fold changes of these lipids in comparison to the controls are represented in the boxplots shown in Fig. 6. Among them, d18:1-S1P was increased significantly in both plasma and urine samples from both GD and GO patients, and the degree of increase was 1.52 (plasma) and 1.53 (urine) times larger in GO than GD. S1P was consistently observed to increase in both plasma and urine samples from patients with GO and therefore, elevation of S1P can be presumed to be an indicator of GO. In addition, while plasma (16:1,18:0)-diacylglycerol (DG) remained unchanged (1.09-fold in GD vs. controls), it was distinctly increased only in GO by approximately 2-fold. AUC value of the receiver operating characteristic analysis (GO vs. GD) for each species is marked at the top of each plot of Fig. 6. Among them, AUCs > 0.80 were observed for d18:1-S1P from both plasma and urine, (16:1,18:0)-DG and 58:7-TG from plasma, and 16:1-LPC and 50:1-TG from urine (ESM Fig. S6). This further supports the aforementioned lipids as potential markers that can distinguish GO from GD at the molecular level.

Conclusions

In this study, 389 plasma and 273 urinary lipids from patients with GD with and without ophthalmopathy were investigated and the changes in lipid levels among the groups were systematically evaluated with statistical methods. While most patients were euthyroid or had mild thyroid function abnormalities under antithyroid drug treatment, their lipidome profile in both plasma and urine samples remained significantly different from healthy controls. Urinary LPC increased significantly by 3- to 10-folds in patients with GD and GO, whereas urinary PC species were found to decrease. Significant differences (> 2-fold, AUC > 0.80 and $p < 0.01$) were observed in a total of 10 plasma and 13 urinary lipids from GD and 19 plasma and 12 urinary lipids from GO compared to healthy controls. Among these, an opposite trend was observed in the variation of TG between plasma and urine samples; plasma TG increased while the urine TG decreased in GD and GO. Moreover, a total of seven lipids varied significantly (> 1.5-fold and $p < 0.01$) in both plasma and urine samples simultaneously in GO patients: 16:0-LPC, 18:0-LPE, 18:1-LPE, 18:0/18:2-PG, d18:1-S1P, d18:1/24:2-SM, and 48:1-TG.

Alteration in plasma and urinary lipids between patients with GO and GD was investigated, and four and eight lipids from plasma and urine, respectively, showed significant changes (> 1.5-fold and $p < 0.01$) between the two groups. Among these, (16:1,18:0)-DG distinctly increased by 1.93-fold in only plasma GO, while it remained unchanged (0.90-

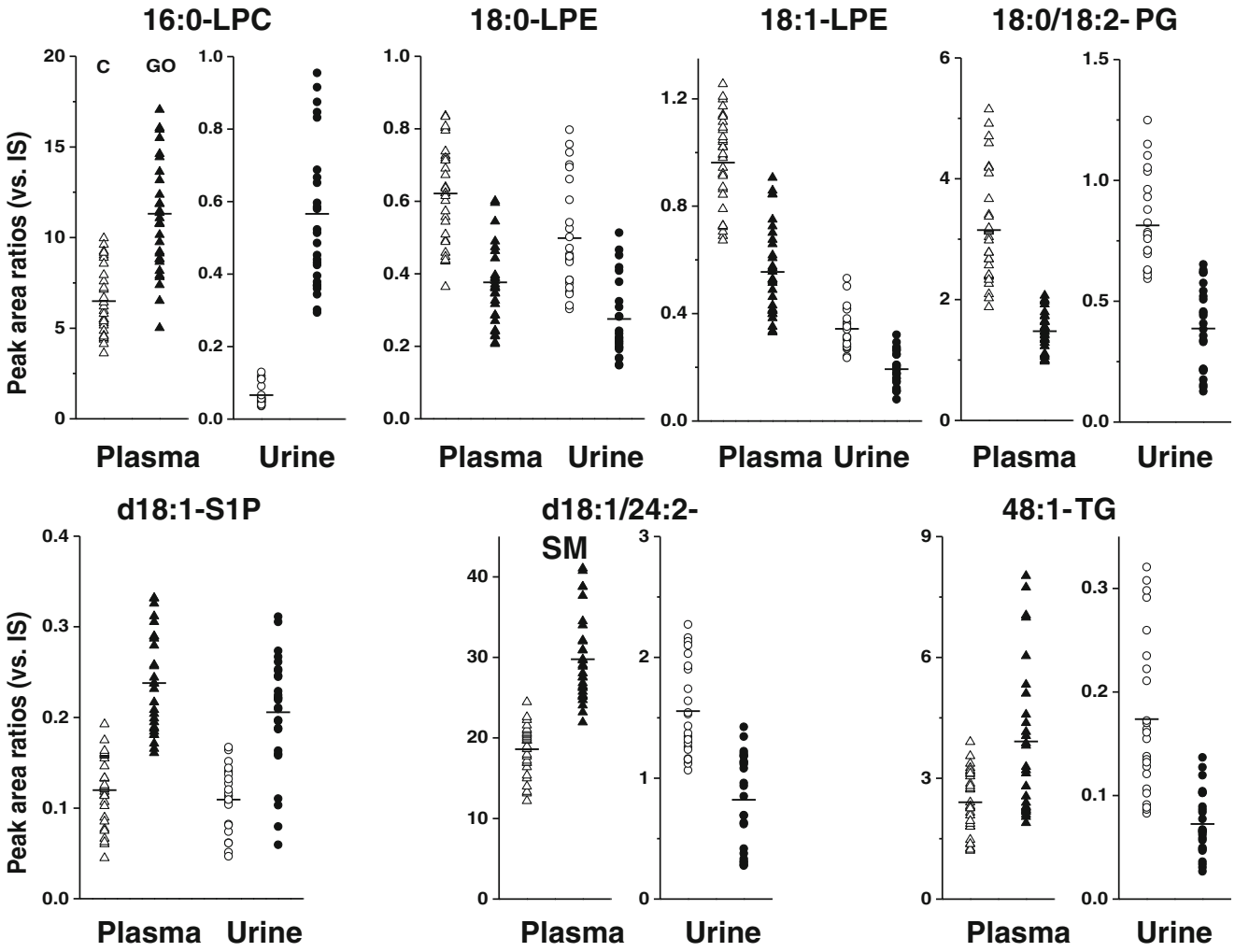

Fig. 5 Peak area ratios for plasma and urine samples. Lipids with significant difference (> 1.5-fold and $p < 0.01$) in both plasma and urine samples, simultaneously, from patients with Graves' ophthalmopathy compared to controls are shown

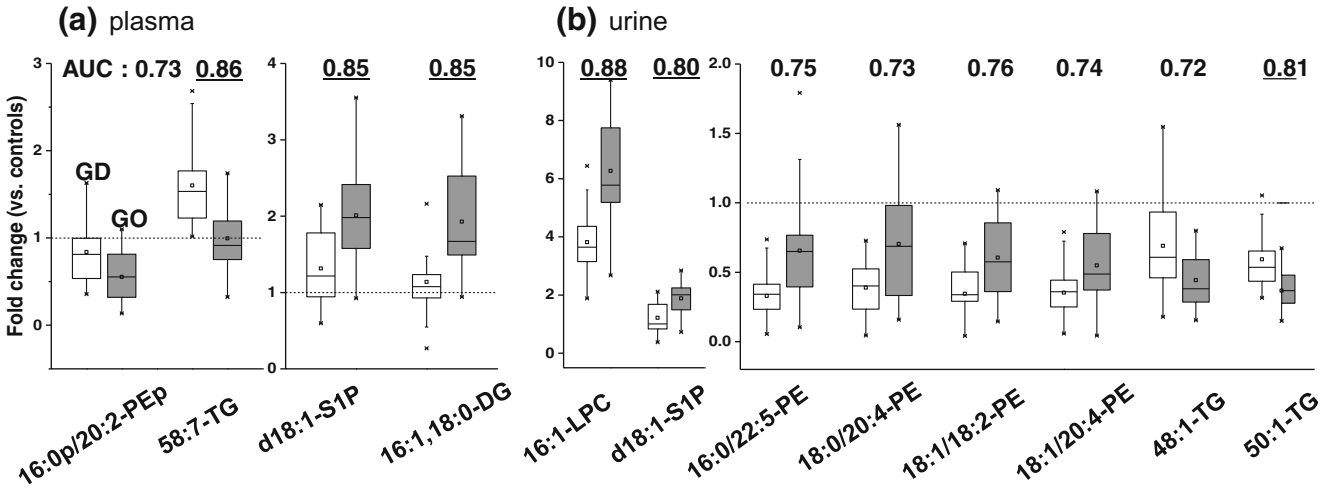

Fig. 6 Fold changes in lipids from (**a**) plasma and (**b**) urine samples based on individual quantification. Lipids that differed significantly (> 1.5-fold with $p < 0.01$) between the patients with Graves' disease and ophthalmopathy are included. The fold changes are the peak area ratios of individual patients to average peak areas of controls ($X_{\text{i from patients}}/\overline{X}_{\text{controls}}$)

and 0.91-fold in urinary GD and GO, respectively) or slightly increased (1.09-fold in plasma GD). d18:1-S1P showed significant changes in both plasma and urine samples of patients with GO, but to a larger degree in GO than in GD. The S1P levels showed consistent and significant increases in both plasma and urine samples of patients with GO and therefore, S1P levels can be concluded as a strong candidate for differentiating between GO and GD.

Acknowledgments This study was supported by a grant (NRF-2015R1A2A1A01004677 to M.H.M) from the National Research Foundation (NRF) of Korea, a grant (2014M3A9B6069341 to E.J.L) from the Bio & Medical Technology Development Program of NRF. S.K.B acknowledges the support of the Yonsei University Research Fund (Post Doc. Researcher Supporting Program) of 2016 (project no.: 2016-12-0230).

Authors' contributions Seul Kee Byeon performed lipidomic experiments, analyzed data, and wrote the manuscript with assistance from Jong Cheol Lee. Se Hee Park contributed to sample collection and data analysis, and wrote the manuscript. Sena Hwang collected samples and contributed to the study design. Cheol Ryong Ku, Dong Yeob Shin, and Jin Sook Yoon contributed to sample collection. Eun Jig Lee designed and supervised the study and contributed to sample collection. Myeong Hee Moon supervised lipidomic analysis and wrote the manuscript. All authors edited the paper.

Compliance with ethical standards

Conflict of interest The authors declare that they have no conflict of interest.

References

1. Hashizume K, Ichikawa K, Sakurai A, Suzuki S, Takeda T, Kobayashi M, et al. Administration of thyroxine in treated Graves' disease: effects on the level of antibodies to thyroid-stimulating hormone receptors and on the risk of recurrence of hyperthyroidism. N Engl J Med. 1991;324(14):947–53.
2. Streetman DD, Khanderia U. Diagnosis and treatment of Graves disease. Ann Pharmacother. 2003;37(7–8):1100–9.
3. Smith TJ, Hegedus L. Graves' disease. N Engl J Med. 2016;375:1552–65.
4. Weetman AP. Graves' disease. N Engl J Med. 2000;343:1236–48.
5. Villadolid MC, Yokoyama N, Izumi M, Nishikawa T, Kimura H, Ashizawa K, et al. Untreated Graves' disease patients without clinical ophthalmopathy demonstrate a high frequency of extraocular muscle (EOM) enlargement by magnetic resonance. J Clin Endocrinol Metab. 1995;80(9):2830–3.
6. Mourits MP, Prummel MF, Wiersinga WM, Koornneef L. Clinical activity score as a guide in the management of patients with Graves' ophthalmopathy. Clin Endocrinol. 1997;47(1):9–14.
7. Di Angelantonio E, Sarwar N, Perry P, Kaptoge S, Ray KK, Thompson A, et al. Major lipids, apolipoproteins, and risk of vascular disease. JAMA. 2009;302:1993–2000.
8. Willer CJ, Sanna S, Jackson AU, Scuteri A, Bonnycastle LL, Clarke R, et al. Newly identified loci that influence lipid concentrations and risk of coronary artery disease. Nat Genet. 2008;40(2):161.
9. Fahy E, Subramaniam S, Murphy RC, Nishijima M, Raetz CR, Shimizu T, et al. Update of the LIPID MAPS comprehensive classification system for lipids. J Lipid Res. 2009;50(Supplement):S9–14.
10. Fahy E, Subramaniam S, Brown HA, Glass CK, Merrill AH, Murphy RC, et al. A comprehensive classification system for lipids. J Lipid Res. 2005;46(5):839–62.
11. Brouwers JF, Vernooij EA, Tielens AG, van Golde LM. Rapid separation and identification of phosphatidylethanolamine molecular species. J Lipid Res. 1999;40(1):164–9.
12. Wright MM, Howe AG, Zaremberg V. Cell membranes and apoptosis: role of cardiolipin, phosphatidylcholine, and anticancer lipid analogues. Biochem Cell Biol. 2004;82(1):18–26.
13. Vesper H, Schmelz EM, Nikolova-Karakashian MN, Dillehay DL, Lynch DV, Merrill AH. Sphingolipids in food and the emerging importance of sphingolipids to nutrition. J Nutr. 1999;129(7):1239–50.
14. Lee ST, Lee JC, Kim JW, Cho SY, Seong JK, Moon MH. Global changes in lipid profiles of mouse cortex, hippocampus, and hypothalamus upon p53 knockout. Sci Rep. 2016;6:36510.
15. Park SM, Byeon SK, Sung H, Cho SY, Seong JK, Moon MH. Lipidomic perturbations in lung, kidney, and liver tissues of p53 knockout mice analyzed by nanoflow UPLC-ESI-MS/MS. J Proteome Res. 2016;15(10):3763–72.
16. Bang DY, Moon MH. On-line two-dimensional capillary strong anion exchange/reversed phase liquid chromatography–tandem mass spectrometry for comprehensive lipid analysis. J Chromatogr A. 2013;1310:82–90.
17. Christianson CC, Johnson CJ, Needham SR. The advantages of microflow LC–MS/MS compared with conventional HPLC–MS/MS for the analysis of methotrexate from human plasma. Bioanalysis. 2013;5(11):1387–96.
18. Friis T, Pedersen LR. Serum lipids in hyper-and hypothyroidism before and after treatment. Clin Chim Acta. 1987;162(2):155–63.
19. Abbas JM, Chakraborty J, Akanji AO, Doi SA. Hypothyroidism results in small dense LDL independent of IRS traits and hypertriglyceridemia. Endocr J. 2008;55(2):381–9.
20. Eckstein AK, Plicht M, Lax H, Neuhäuser M, Mann K, Lederbogen S, et al. Thyrotropin receptor autoantibodies are independent risk factors for Graves' ophthalmopathy and help to predict severity and outcome of the disease. J Clin Endocrinol Metab. 2006;91(9):3464–70.
21. Byeon SK, Lee JY, Moon MH. Optimized extraction of phospholipids and lysophospholipids for nanoflow liquid chromatography-electrospray ionization-tandem mass spectrometry. Analyst. 2012;137(2):451–8.
22. Lim S, Byeon SK, Lee JY, Moon MH. Computational approach to structural identification of phospholipids using raw mass spectra from nanoflow liquid chromatography–electrospray ionization–tandem mass spectrometry. J Mass Spectrom. 2012;47(8):1004–14.
23. Cajka T, Fiehn O. Increasing lipidomic coverage by selecting optimal mobile-phase modifiers in LC–MS of blood plasma. Metabolomics. 2016;12(2):34.
24. Lee JC, Kim IY, Son Y, Byeon SK, Yoon DH, Son JS, et al. Evaluation of treadmill exercise effect on muscular lipid profiles of diabetic fatty rats by nanoflow liquid chromatography–tandem mass spectrometry. Sci Rep. 2016;6:29617.
25. Maceyka M, Harikumar KB, Milstien S, Spiegel S. Sphingosine-1-phosphate signaling and its role in disease. Trends Cell Biol. 2012;22(1):50–60.
26. Hannun YA, Obeid LM. The ceramide-centric universe of lipid-mediated cell regulation: stress encounters of the lipid kind. J Biol Chem. 2002;277(29):25847–50.
27. Kolesnick R. The therapeutic potential of modulating the ceramide/sphingomyelin pathway. J Clin Invest. 2002;110(1):3–8.
28. Prieur X, Huby T, Coste H, Schaap FG, Chapman MJ, Rodríguez JC. Thyroid hormone regulates the hypotriglyceridemic gene APOA5. J Biol Chem. 2005;280(30):27533–43.

29. Rensen PC, van Dijk KW, Havekes LM. Apolipoprotein AV: low concentration, high impact. Arterioscler Thromb Vasc Biol. 2005;25:2445–7.
30. Schmitz G, Ruebsaamen K. Metabolism and atherogenic disease association of lysophosphatidylcholine. Atherosclerosis. 2010;208(1):10–8.
31. Lee JY, Lim S, Park S, Moon MH. Characterization of oxidized phospholipids in oxidatively modified low density lipoproteins by nanoflow liquid chromatography-tandem mass spectrometry. J Chromatogr A. 2013;1288:54–62.
32. Lee JY, Byeon SK, Moon MH. Profiling of oxidized phospholipids in lipoproteins from patients with coronary artery disease by hollow fiber flow field-flow fractionation and nanoflow liquid chromatography–tandem mass spectrometry. Anal Chem. 2014;87(2):1266–73.